

8 **Measurement of charged particle production in deep-inelastic**
9 ***ep* scattering at $\sqrt{s} = 225\text{GeV}$ at HERA**

H1 Collaboration

Abstract

Charged particle production is measured in deep inelastic ep scattering at $\sqrt{s} = 225\text{ GeV}$ with the H1 detector at HERA. The kinematic range of the analysis covers low photon virtualities, $5 < Q^2 < 10\text{ GeV}^2$, and medium to high values of inelasticity y , $0.35 < y < 0.8$. The analysis is performed in the virtual photon-proton centre-of-mass system. The charged particle production cross sections is investigated double-differentially as a function of pseudorapidity η^* and transverse momentum p_T^* in the range $0 < \eta^* < 3.5$ and $p_T^* < 10\text{ GeV}$. The data are compared to different phenomenological models.

1 Introduction

Recently, it was found that the shape of charged particle transverse momentum distributions measured in baryon-baryon interactions is distinctly different from that observed in gamma-gamma interactions [1]. This is an indication for possible difference in underlying dynamics of hadron production for these two types of particle collisions. At HERA both photoproduction and DIS processes are mediated by photon exchange, and therefore it provides an unique possibility to study the intermediate case of baryon-photon interactions. Naïvely one would expect to observe a change in the hadron production dynamics at central rapidities in photon-proton (γ^*p) centre-of-mass system.

Due to the strong asymmetry in the beam energies of electron and proton beams at HERA the previous inclusive hadron production measurements [2] had only limited access to the central rapidity region in the γ^*p frame. This region can be studied more easily by using the data collected at reduced proton beam energy and by restricting the event kinematics to large values of the γ^*p rest mass W_{γ^*p} .

2 Event Selection

2.1 DIS and detector level selection

In 2007 the HERA ep -collider has also been run at reduced proton beam energy ($E_p = 460$ GeV) for three months in which the H1 experiment has collected data corresponding to an integrated luminosity of 12.45 pb^{-1} . These data are used in the present analysis of the charged particle spectra shape in the γ^*p rest frame.

DIS events are recorded using triggers based on electromagnetic energy deposits in the SpaCal calorimeter. The trigger efficiency is determined using independently triggered data. For DIS events the trigger efficiency is determined to be almost 100% in the kinematic region of the analysis. The scattered lepton, defined by the most energetic SpaCal cluster, is required to have an energy E_e larger than 3.4 GeV. The kinematical phase space is defined by $5 < Q^2 < 10 \text{ GeV}^2$ and $0.35 < y < 0.8$, corresponding to the geometric acceptance of the SpaCal.

Several cuts are applied to suppress photoproduction background. The electron identification selection criteria are designed to have a high efficiency for the signal while rejecting significantly the background. A detailed description of these cuts can be found elsewhere [3].

2.2 Tracks Selection

The tracks used in the analysis are measured in the central tracking detector (CTD). The reconstruction in the central region is based on two drift chambers, CJC1 and CJC2. The tracks are used to define the event vertex. In this analysis only tracks from the primary vertex are considered.

In order to provide a higher efficiency of the track reconstruction, the following cuts are applied:

- 56 • The transverse momentum p_T of a track has to be larger than 0.12 GeV.
- 57 • The polar angular range of a track is required to be $20^\circ < \theta < 160^\circ$.
- 58 • Tracks are required to have a radial length L (the radial distance between the first and the
- 59 last hit) larger than 10 cm for the full θ range to ensure good momentum resolution.
- 60 • Starting point of a track is required to be in CJC1.

61 2.3 Definition of experimental observables

62 The results of this analysis are presented in the γ^*p centre-of-mass frame, to minimise the effect
63 of the transverse boost from the virtual photon. The transformation to the this frame is recon-
64 structed with the knowledge of the kinematic variables Q^2 and y . The transverse momentum
65 and pseudorapidity of charged particles in this frame are labeled as p_T^* and η^* . In the photon-
66 proton centre-of-mass frame the pseudorapidity is defined as $\eta^* = \ln(\tan(\theta^*/2))$, where θ^*
67 is the polar angle of the track with respect to the virtual photon direction, i.e. the positive z^*
68 direction. All hadronic final state particles with $\eta^* > 0$ belong to the current hemisphere, and
69 all particles with $\eta^* < 0$ are assigned to the target or proton remnant hemisphere.

70 The transverse momenta of charged particles are studied in the pseudorapidity region $0 <$
71 $\eta^* < 3.5$ which is divided into seven equal intervals. This division in η^* -intervals is made
72 in order to investigate how the charged particle p_T^* -spectrum changes with η^* going form the
73 photon direction to the central fragmentation region. The target region, $\eta^* < 0$, is not accessible
74 in this analysis. The transverse momenta of charged particles is measured for $p_T^* > 150$ MeV
75 in order to minimize the influence of the boost to virtual photon-proton centre-of-mass frame.

76 2.4 Cross Section Definition

77 The double differential cross section is defined at Born level by the following equation

$$\frac{d^2\sigma}{dp_T^{*2}d\eta^*} = \frac{N_{sig}}{\mathcal{L} \cdot 2p_T^* \cdot \Delta p_T^* \cdot \Delta \eta^* \cdot A \cdot \varepsilon_1 \dots \varepsilon_n} \cdot RC \quad (1)$$

78 where \mathcal{L} is the luminosity, $\Delta \eta^*$ and $\Delta p_T^{*2} = 2 \cdot p_T^* \cdot \Delta p_T^*$ are the bin widths, ε_i is the efficiency of
79 a given cut i , A - the acceptance correction measured at the reconstructed level in the radiative
80 Monte Carlo (with the initial and final state radiation turned on) to the cross section at the
81 generator level:

$$A = \frac{N_{rec}^{rad}}{N_{gen}^{rad}}, \quad (2)$$

82 and RC is a radiative correction factor extracted using the ratio of the MC calculated cross
83 section excluding initial and final state radiation to that with radiation included:

$$RC = \frac{\sigma_{gen}^{norad}}{\sigma_{gen}^{rad}}. \quad (3)$$

84 The bin-center correction is also performed assuming the points to lie in the geometrical
85 centers of p_T^* bins. The DJANGO MC was used to correct the data.

3 Results and Discussions

The measured cross section $d\sigma/d\eta^*$ for charged particles with $p_T^* > 0$ GeV is shown in figure 1 together with the predictions DJANGO and RAPGAP normalised to the data. The shape of the pseudorapidity distribution is described by Monte Carlo rather well.

The double differential cross sections $d^2\sigma/dp_T^{*2}d\eta^*$ for charged particles are shown in figure 2 together with the absolute predictions from DJANGO and RAPGAP. The ratio MC over data is shown in figure 3 applying the same normalisation factors to the models predictions as used in figure 1 independently of η^* . Although these models provide a rather good description of the cross section in η^* (figure 1) they fail to describe the shape of the transverse momentum spectra of the charged particles (figure 3).

To study the hadroproduction dynamics we use the approximation which has been proposed recently [1]. This approach suggests that the shape of the particle production p_T^* spectrum can be described by the sum of an exponential (Boltzmann-like) and a power-law statistical distributions:

$$\frac{d\sigma}{p_T^* dp_T^*} = A_e \exp(-E_{Tkin}/T_e) + \frac{A}{(1 + \frac{p_T^{*2}}{T^2 \cdot N})^N}, \quad (4)$$

where $E_{Tkin} = \sqrt{p_T^{*2} + M^2} - M$ with M equal to the produced hadron mass. A_e, A, T_e, T, N are free parameters to be determined by fit to the data. For charged hadron spectra a hadron mass is assumed to be equal to the pion mass. Detailed arguments for this particular choice are given in [1] and a phenomenological explanation of the formula (4) has been recently given in [4]. The parameterisation in equation (4) provides a much better description of the data than the one traditionally used [5].

The double differential cross sections $d^2\sigma/dp_T^{*2}d\eta^*$ are shown for seven η^* bins in figure 4 together with the fit (4).

The relative contribution of the exponential and power-law terms of the approximation (4) can be characterised by ratio R of the power-law term alone to the parameterisation function integrated over p_T^* . The power-law term can be calculated in the following way:

$$\int_0^\infty \frac{A}{(1 + \frac{p_T^{*2}}{T^2 N})^N} dp_T^{*2} = \frac{ANT^2}{N-1}.$$

The exponential:

$$\begin{aligned} A_e \int_0^\infty e^{-\frac{E_{Tkin}}{T_e}} dp_T^{*2} &= A_e \int_0^\infty e^{-\frac{m - \sqrt{p_T^{*2} + m^2}}{T_e}} dp_T^{*2} \\ z &= \sqrt{p_T^{*2} + m^2} - m \\ dz &= \frac{dp_T^{*2}}{\sqrt{p_T^{*2} + m^2}} = \frac{dp_T^{*2}}{m + z} \\ (m + z)dz &= dp_T^{*2} \\ A_e \int_0^\infty e^{-\frac{m - \sqrt{p_T^{*2} + m^2}}{T_e}} dp_T^{*2} &= A_e \int_0^\infty e^{-\frac{z}{T_e}} 2(m + z)dz = A_e(2mT_e + 2T_e^2). \end{aligned}$$

112 Therefore, the relative contribution R can be expressed by the formula:

$$R = \frac{AnT^2}{AnT^2 + A_e(2MT_e + 2T_e^2)(n - 1)}. \quad (5)$$

113 In figure 5 the parameters of the fit function and the relative contribution R of the power-law
114 type distribution to the charged particle production spectra (equation (5)) are shown as function
115 of the charged particle rapidity (η^*). Close to the virtual photon direction (large values of η^*)
116 the p_T^* spectrum can be described by a power-law term only, while at central rapidities the
117 data require a significant exponential (Boltzmann-like) contribution. Moreover, the smaller η^*
118 the larger the exponential statistical contribution is required to describe the inclusive charged
119 particle spectrum. Note, that in the pp interaction at about the same collision energy as here for
120 γ^*p at HERA the data require only about 30% of the power-law type contribution to the charged
121 particle spectrum measured at central rapidities, while the residual 70% of the particle spectrum
122 is described by the exponential contribution [1]. Thus, we observe that the particle production
123 regime changes when particle rapidity values approach the proton hemisphere in the rapidity
124 space of DIS events.

125 4 Conclusion

126 The first measurement of charged particle production spectra in ep collisions at reduced pro-
127 ton beam energy $E_p = 460$ GeV with the H1 detector in the virtual photon-proton centre-of-
128 mass frame was performed. The kinematic range of the analysis covers low photon virtualities,
129 $5 < Q^2 < 10$ GeV², and from medium to high values of inelasticity, $0.35 < y < 0.8$. The
130 double differential charged particle production cross sections $d^2\sigma/dp_T^{*2}d\eta^*$ are measured in the
131 pseudorapidity region $0 < \eta^* < 3.5$ in seven equal bins. The measured transverse momentum
132 distributions show different shape, depending on the η^* value. The Monte Carlo models RAP-
133 GAP and DJANGO describe the shape of the cross section in η^* but both fail to describe the
134 shape of the cross section $d^2\sigma/dp_T^{*2}d\eta^*$.

135 In order to investigate the change in hadroproduction dynamics with η^* the data are ap-
136 proximated by the recently introduced approach (4). This parameterisation provides a much
137 better description of the experimental data than those traditionally used. Moreover, the ob-
138 served change in the particle production regime when particle rapidity values approach the
139 proton hemisphere in the rapidity space of DIS events, is rather well explained by the newly
140 introduced qualitative model [4].

141 References

- 142 [1] A. A. Bylinkin and A. A. Rostovtsev, “Parametrization of the shape of hadron-production
143 spectra in high-energy particle interactions,” Phys. Atom. Nucl. **75** (2012) 999 [Yad. Fiz.
144 **75** (2012) 1060].

- 145 [2] C. Adloff *et al.* [H1 Collaboration], "Measurement of Charged Particle Transverse Mo-
146 mentum Spectra in Deep Inelastic Scattering", Nucl. Phys. **B 485** (1996)3 ;
147 C. Alexa *et al.* [H1 Collaboration], "Measurement of Charged Particle Spectra in Deep-
148 Inelastic ep Scattering at HERA", submitted to Eur. Phys. J. C, [arxiv:1302.1321].
- 149 [3] F. D. Aaron *et al.* [H1 Collaboration], "Measurement of the Inclusive $e\pm p$ Scattering
150 Cross Section at High Inelasticity y and of the Structure Function F_L ," Eur. Phys. J. **C 71**
151 (2011) 1579 [arXiv:1012.4355].
- 152 [4] A. A. Bylinkin and A. A. Rostovtsev, "A photon-proton marriage," arXiv:1209.0958 [hep-
153 ph].
- 154 [5] R. Hagedorn, Riv. Nuovo Cim. **6** (1983) 1.

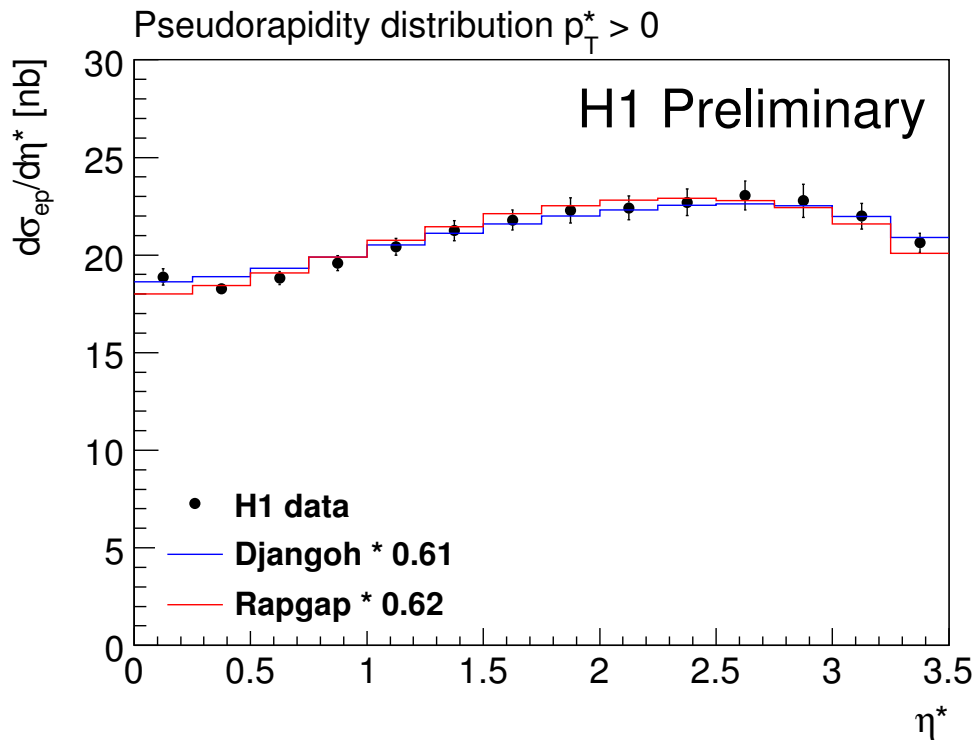


Figure 1: The measured differential ep cross section $d\sigma/d\eta^*$ for inclusive production of charged particles. Particles with a $p_T^* > 0$ GeV are considered. The lines represent the normalized prediction of DJANGO and RAPGAP respectively.

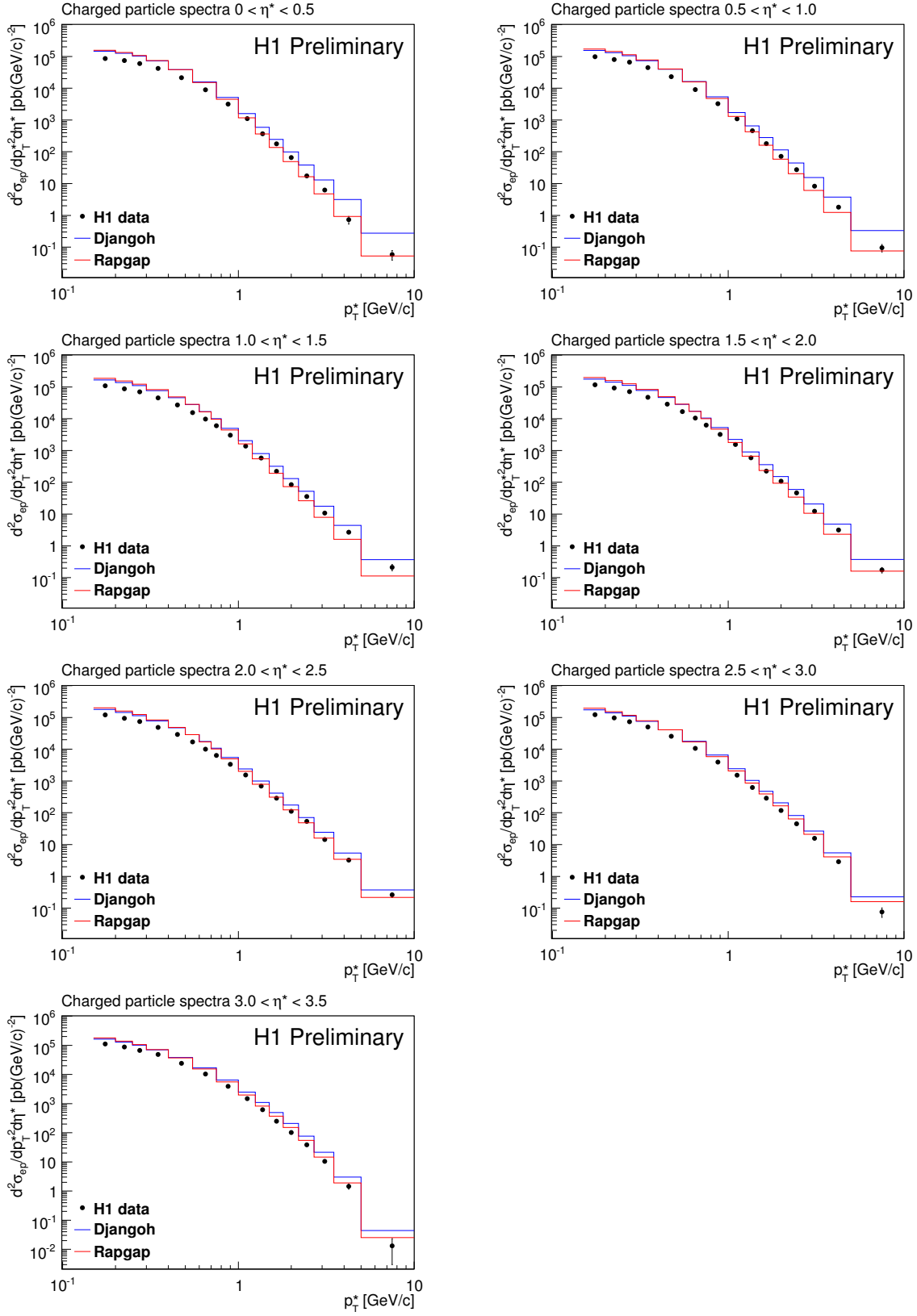


Figure 2: The measured charged particle double differential cross section $d^2\sigma/dp_T^2 d\eta$ for seven η^* intervals together with DJANGO and RAGGAP predictions.

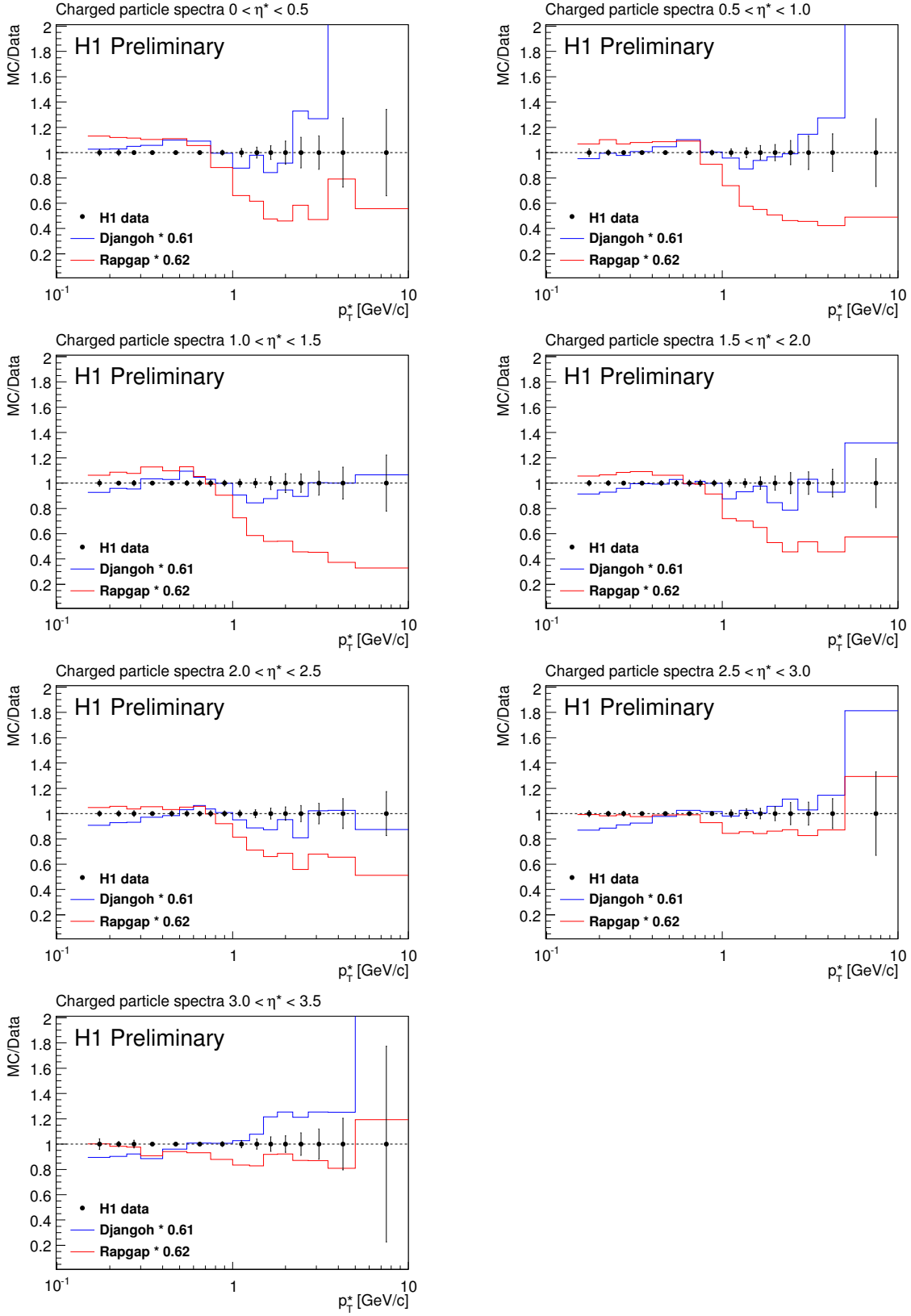


Figure 3: The ratios of normalised MC over data using the same as used in figure 1 for seven η^* intervals.

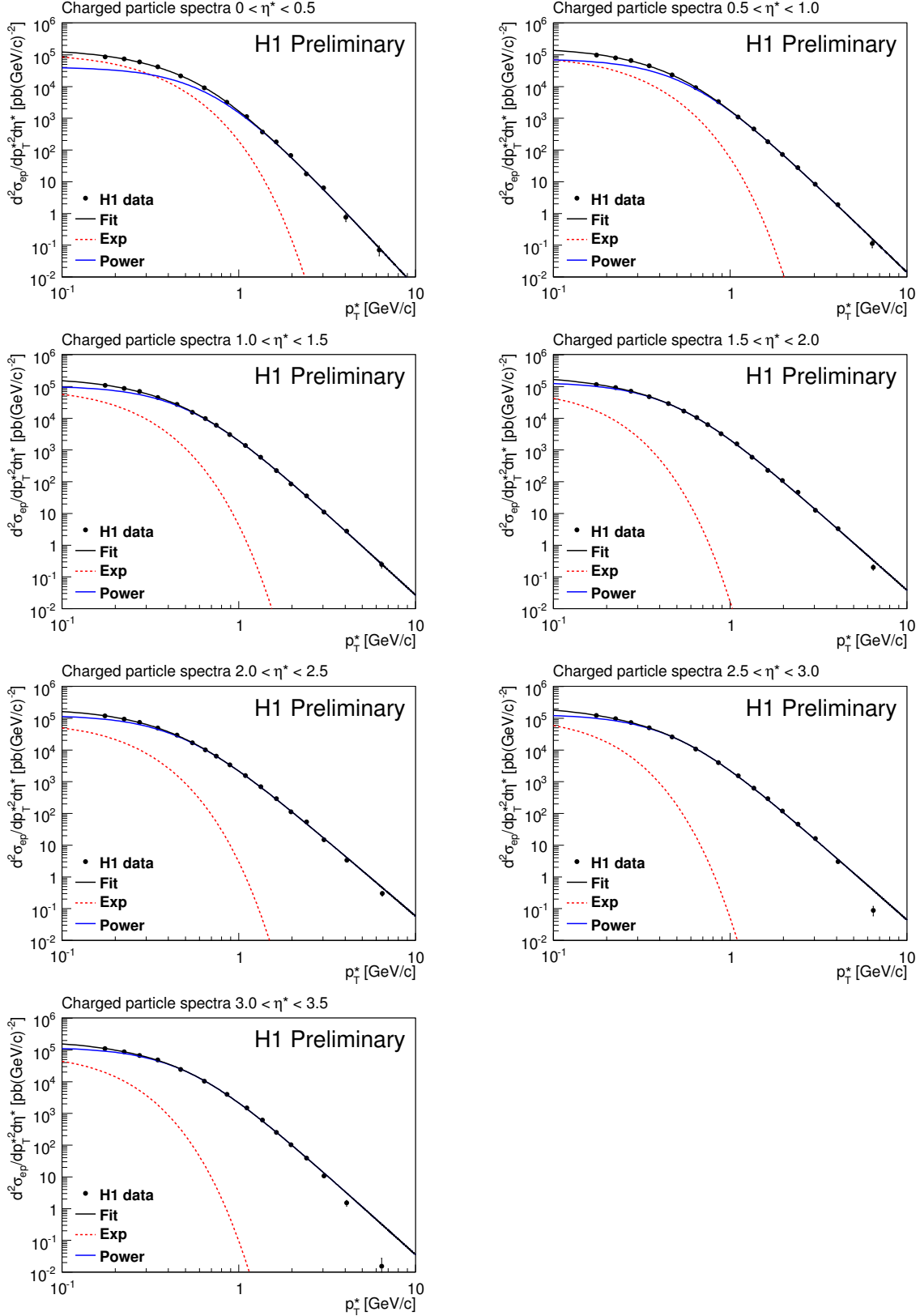


Figure 4: Double differential charged particle cross section $d^2\sigma/dp_T^2d\eta$ for seven η^* intervals together results from the fits of the function (4): the red line shows the exponential term and the blue one - the power law. Bin-center correction is performed.

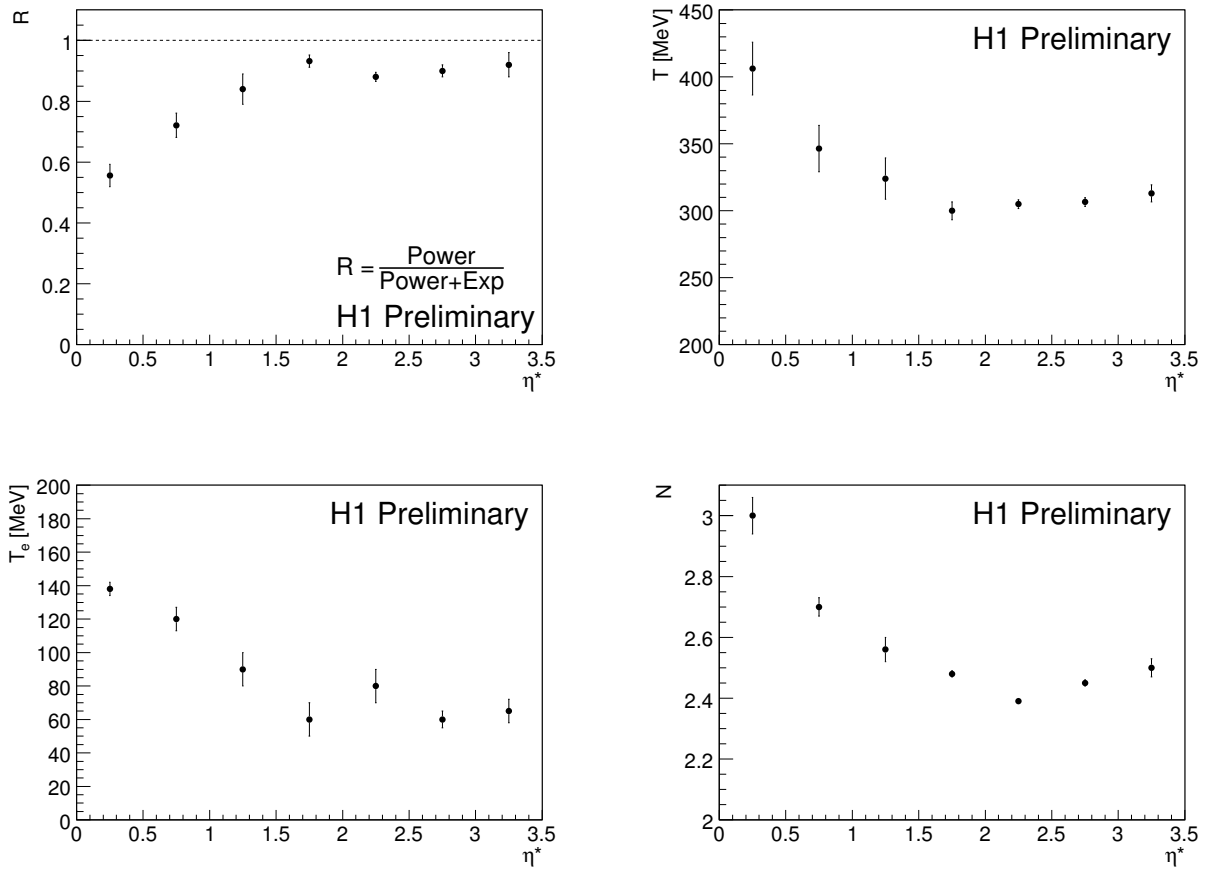


Figure 5: Contribution R of the power law term and fitted parameters of (4) as function of pseudorapidity (η^*). The data points used for the fits included uncorrelated systematics.